One-Electron Oxidations of the Methyldiphenylphosphonium Cyclopentadienylide Complexes M(η^5-$C_5H_4PMePh_2$)$(CO)_3$ (M = Cr, Mo, W): Formation and Dimerization of the 17-Electron, Metal-Centered Radicals [M(η^5-$C_5H_4PMePh_2$)$(CO)_3$]$^+$

John H. Brownie and Michael C. Baird*

Department of Chemistry, Queen's University, Kingston, Ontario K7L 3N6, Canada

Derek R. Laws and William E. Geiger

Department of Chemistry, University of Vermont, Burlington, Vermont 05405

Received July 10, 2007

Electrochemical oxidations of the group 6 metal complexes M(η^5-$C_5H_4PMePh_2$)$(CO)_3$ (M = Cr (**1**), Mo (**2**), W (**3**)) occur via one-electron processes at potentials that are highly positive of the values previously observed for the analogous 18-electron anions [M(η^5-C_5H_5)$(CO)_3$]$^-$. A value of +0.44 V was determined for the electronic effect of the R = $[PMePh_2]^+$ group compared to R = H in a C_5H_4R ligand, making it one of the most strongly electron-withdrawing substituents known. On the basis of the experimentally determined oxidation potentials and observations that the oxidized species were long-lived, bulk oxidations of **1**, **2**, and **3** by $[FeCp_2][B(C_6F_5)_4]$ were carried out to give the crystalline, dimeric products [M(η^5-$C_5H_4PMePh_2$)$(CO)_3$]$_2$[$B(C_6F_5)_4$]$_2$ (M = Cr ($\mathbf{1_2}^{2+}$), Mo ($\mathbf{2_2}^{2+}$), and W ($\mathbf{3_2}^{2+}$)). These were isolated analytically pure and were characterized by IR (solid state and solution) and NMR (^{1}H, ^{13}C, ^{19}F, ^{31}P) spectroscopy, high-resolution mass spectrometry, and crystallographically. The dimers all contain metal−metal bonds that are comparable in length with or longer than the metal−metal bonds in the isoelectronic, neutral η^5-C_5H_5 and η^5-C_5Me_5 analogues, and the metal−metal bond in $\mathbf{1_2}^{2+}$ is the longest nonbridged Cr−Cr bond known. As a result of the apparent weakness of its Cr−Cr bond, $\mathbf{1_2}^{2+}$ dissociates significantly in solution to the paramagnetic radical cation $\mathbf{1}^+$; the ^{1}H NMR spectrum of this complex in THF at 298 K exhibits characteristic C_5H_4 resonances at δ 26.08 and 13.62.

Introduction

We have recently reported the synthesis and reactivity of a series of group 6 complexes of methyldiphenylphosphonium cyclopentadienylide ($C_5H_4PMePh_2$), M(η^5-$C_5H_4PMePh_2$)$(CO)_3$ (M = Cr (**1**), Mo (**2**), W (**3**)).[1] This ligand belongs to an as yet uncommon class of phosphonium cyclopentadienylides, first reported in 1956 by Ramirez and Levy,[2a] who described the synthesis of triphenylphosphonium cyclopentadienylide, $C_5H_4PPh_3$.[2b−f] They found *inter alia* that this ylide is unusually inert, for instance being unreactive with ketones, and they attributed its unusual stability to the charge delocalization implied by resonance structure **b**.

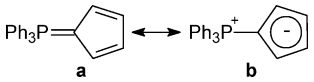

a **b**

Further evidence for extensive delocalization of the π electron density was found in the relatively high dipole moment of 7.0 D,[2c] in the crystal structure, which showed significant shortening of the P−C_5H_4 bond,[2g] and in the ^{13}C NMR spectrum, which showed an unusually high-field chemical shift for the ylide carbon and a P−C(ylide) coupling constant typical of an aliphatic carbon−P bond.[2h] Our more recent crystallographic and spectroscopic data and DFT calculations on the C_5H_4-$PMePh_2$ system strongly confirmed the importance of the cyclopentadienyl-like structure such as **b** for free $C_5H_4PMePh_2$ and, even more so, when $C_5H_4PMePh_2$ is coordinated in η^5-fashion as in **1**, **2**, and **3**.[1]

The spectroscopic data for complexes **1**−**3** also demonstrated that while the cyclopentadienylide ligand is intermediate in electron donor properties between those of neutral η^6-arenes and the anionic η^5-C_5H_5 ligand, its properties lie rather closer to that of the latter.[1] Therefore, in view of the equilibria that exist between the metal−metal bonded dimers [Cr(η^5-C_5H_5)-$(CO)_3]_2$ and [Cr(η^5-C_5Me_5)$(CO)_3]_2$ and their corresponding 17-electron, metal-centered persistent radicals,[3a,b,f,h−k,o,t−w] we wondered if compounds **1**−**3** might undergo one-electron oxidations to give the isoelectronic, persistent cationic metal-centered radicals [M(η^5-$C_5H_4PMePh_2$)$(CO)_3$]$^+$ (M = Cr ($\mathbf{1}^+$), Mo ($\mathbf{2}^+$), W ($\mathbf{3}^+$)) and, if so, to what extent would they dimerize to the dicationic, metal−metal bonded species [M(η^5-C_5H_4-$PMePh_2$)$(CO)_3]_2^{2+}$ (M = Cr ($\mathbf{1_2}^{2+}$), Mo ($\mathbf{2_2}^{2+}$), W ($\mathbf{3_2}^{2+}$)).

There seems to exist only a single prior publication dealing with this type of redox chemistry. Cashman and Lalor reported in 1971 that Mo(η^5-$C_5H_4PPh_3$)$(CO)_3$ is oxidized by tris(*p*-bromophenyl)amminium hexachloroantimonate to give the

(1) Brownie, J. H.; Baird, M. C.; Schmider, H. L. *Organometallics* **2007**, *26*, 1433.

(2) (a) Ramirez, F.; Levy, S. *J. Org. Chem.* **1956**, *21*, 488. (b) Ramirez, F.; Levy, S. *J. Org. Chem.* **1956**, *21*, 1333. (c) Ramirez, F.; Levy, S. *J. Am. Chem. Soc.* **1957**, *79*, 67. (d) Ramirez, F.; Dershowitz, S. *J. Org. Chem.* **1957**, *22*, 41. (e) Ramirez, F.; Levy, S. *J. Am. Chem. Soc.* **1957**, *79*, 6167. (f) Ramirez, F.; Levy, S. *J. Org. Chem.* **1958**, *23*, 2035. (g) Ammon, H. L.; Wheeler, G. L.; Watts, P. H. *J. Am. Chem. Soc.* **1973**, *95*, 6158. (h) Gray, G. A. *J. Am. Chem. Soc.* **1973**, *95*, 7736. (i) For a recent computational study, see: Laavanya, P.; Krishnamoorthy, B. S.; Panchanatheswaran, K.; Manoharan, M. *J. Mol. Struct. (THEOCHEM)* **2005**, *716*, 149.

10.1021/om700688p CCC: $37.00
Publication on Web 10/19/2007

metal−metal bonded, dicationic complex $[Mo(\eta^5\text{-}C_5H_4PPh_3)(CO)_3]_2^{2+}$, identified on the basis of elemental analysis and its IR spectrum.[4] However, group 6 metal compounds containing other ligands provide a rich array of cationic 17-electron complexes.[5] For instance oxidation of $M(CO)_6$ (M = Cr, Mo, W) gives the unstable cations $[M(CO)_6]^+$, which have lifetimes on the order of seconds (Cr) or are too unstable to isolate (Mo, W).[6] Substituted derivatives $M(CO)_{6-n}L_n$, $M(CO)_4L-L$, and $M(CO)_2(L-L)_2$ (n = 1−3; L, L−L = mono- and bidentate tertiary phosphines), on the other hand, yield more thermally stable oxidized complexes, and these have been better characterized.[7] While oxidation of compounds of the type $Cr(\eta^6\text{-arene})(CO)_3$ yields products that are labile[8] unless they are generated in the presence of weakly coordinating anions,[8e] several phosphine-substituted complexes $[M(\eta^6\text{-arene})(CO)_2L]^+$ (M = Cr) were found to be stable enough to isolate and characterize.[8] However, none of these cationic, metal-centered radicals appear to form dicationic dimers.

Of greater relevance here, however, the anionic group 6 tricarbonyl complexes $[M(\eta^5\text{-}C_5H_5)(CO)_3]^-$ and $[M(\eta^5\text{-}C_5Me_5)(CO)_3]^-$ (M = Cr, Mo, W) are readily oxidized to the neutral metal-centered radicals $M(\eta^5\text{-}C_5H_5)(CO)_3$ and $M(\eta^5\text{-}C_5Me_5)(CO)_3$, which dimerize to give the metal−metal bonded complexes $[M(\eta^5\text{-}C_5H_5)(CO)_3]_2$ and $[M(\eta^5\text{-}C_5Me_5)(CO)_3]_2$.[3] Although the molybdenum and tungsten dimers do not dissociate in solution,[3] the chromium dimers dissociate as mentioned above to give the corresponding persistent 17-electron radical monomers.[3] We have therefore embarked on a complementary examination of the redox chemistry of compounds **1**−**3**, finding that they do indeed undergo oxidation to the corresponding 17-electron, metal-centered radicals $[M(\eta^5\text{-}C_5H_4PMePh_2)(CO)_3]^+$ where M = Cr ($\mathbf{1}^+$), Mo ($\mathbf{2}^+$), and W ($\mathbf{3}^+$), and that these in turn dimerize to the corresponding metal-bonded complexes $[M(\eta^5\text{-}C_5H_4PMePh_2)(CO)_3]_2^{2+}$ ($\mathbf{1_2}^{2+}$, $\mathbf{2_2}^{2+}$, and $\mathbf{3_2}^{2+}$, respectively). As with the above-mentioned compounds $[M(\eta^5\text{-}C_5H_5)(CO)_3]_2$ and $[M(\eta^5\text{-}C_5Me_5)(CO)_3]_2$, we find that the chromium dimer $\mathbf{1_2}^{2+}$ dissociates extensively in solution to the persistent radical monomer $\mathbf{1}^+$, but that the heavier metal analogues $\mathbf{2_2}^{2+}$ and $\mathbf{3_2}^{2+}$ dissociate very little, if at all.

Experimental Section

All syntheses were carried out under a dry, deoxygenated argon atmosphere using standard Schlenk techniques or under nitrogen in an MBraun Labmaster glovebox. Argon was deoxygenated by passage through a heated column of BASF copper catalyst and then dried by passing through a column of 4 Å molecular sieves. NMR spectra were recorded using Bruker AV 300, AV 500, and AV 600 spectrometers; all ^1H and $^{13}C\{^1H\}$ NMR spectra are referenced to carbons or residual protons present in the deuterated solvents with respect to TMS at δ 0, while ^{31}P NMR spectra are referenced to external 85% H_3PO_4. Elemental analyses were carried out by Canadian Microanalytical Service Ltd., Delta, B.C. IR spectra were acquired on a Perkin-Elmer Spectrum One FT-IR spectrometer at a spectral resolution of 4 cm^{-1} (Queen's) or on a ATI-Mattson Infinity Series FT-IR spectrometer using Winfirst software and operating at a resolution of 4 cm^{-1} (Vermont). A Remspec ZnSe fiber-optic cable terminating in a gold reflective disk was used for *in situ* attenuated total reflectance measurements;[9] a spectral window from 1500 to 2200 cm^{-1} was available under the experimental conditions. Electrospray mass spectrometry (ES-MS) data were collected in the Mass Spectrometry Facility at Queen's on an Applied Biosystems/MDS Sciex QSTAR XL QqTOF mass spectrometer.

The CH_2Cl_2, THF, and hexanes used for syntheses were purchased from Aldrich in 18 L reservoirs packaged under nitrogen and were dried by passage through columns of activated alumina (Innovative Technology Solvent Purification System). THF, Et_2O, and CH_2Cl_2 were then stored over 4 Å molecular sieves to result in residual water concentrations that were lower than 20 ppm. Deuterated NMR solvents (Cambridge Isotope Laboratories, Inc. or CDN Isotopes) were degassed under vacuum and dried by passage through a small column of activated alumina before being stored over 4 Å molecular sieves. Most chemicals were obtained from Aldrich or Strem and were used as received or were purified by established procedures. The compounds $M(\eta^5\text{-}C_5H_4PMePh_2)(CO)_3$ (M = Cr, Mo, W)[1] and $[FeCp_2][B(C_6F_5)_4]$[10] were synthesized according to the literature.

All electrochemical experiments were conducted (Vermont) using Princeton Applied Research models PAR-173 and PAR-273 potentiostats interfaced to personal computers. For these experiments, CH_2Cl_2 was dried over CaH_2, distilled under nitrogen, and purified further by vacuum transfer from fresh drying agent prior to use, while $[NBu_4][B(C_6F_5)_4]$ was prepared by metathesis of $[NBu_4]Br$

(3) (a) Adams, R. D.; Collins, D. E.; Cotton, F. A. *J. Am. Chem. Soc.* **1974**, *96*, 749. (b) Landrum, J. T.; Hoff, C. D. *J. Organomet. Chem.* **1985**, *282*, 215. (c) Hackett, P.; O'Neill, P. S.; Manning, A. R. *J. Chem. Soc., Dalton Trans.* **1974**, 1625. (d) Madach, T.; Vahrenkamp, H. *Z. Naturforsch.* **1979**, *34b*, 573. (e) Goh, L.-Y.; D'Aniello, M. J.; Slater, S.; Muetterties, E. L.; Tavanaiepour, I.; Chang, M.I.; Fredrich, M. F.; Day, V. W. *Inorg. Chem.* **1979**, *18*, 192. (f) Cooley, N. A.; Watson, K. A.; Fortier, S.; Baird, M. C. *Organometallics* **1986**, *5*, 2563. (g) Keller, H. J. *Z. Naturforsch.* **1968**, *23b*, 133. (h) Madach, T.; Vahrenkamp, H. *Z. Naturforsch.* **1978**, *33b*, 1301. (i) McLain, S. J. *J. Am. Chem. Soc.* **1988**, *110*, 643. (j) Cooley, N. A.; MacConnachie, P. T. F.; Baird, M. C. *Polyhedron* **1988**, *7*, 1965. (k) Jaeger, T. J.; Baird, M. C. *Organometallics* **1988**, *7*, 2074. (l) Wrighton, M. S.; Ginley, D. S. *J. Am. Chem. Soc.* **1975**, *97*, 4246. (m) Hughey, J. L.; Bock, C. R.; Meyer, T. J. *J. Am. Chem. Soc.* **1975**, *97*, 4440. (n) Laine, R. M.; Ford, P. C. *Inorg. Chem.* **1977**, *16*, 388. (o) Watkins, W. C.; Jaeger, T.; Kidd, C. E.; Fortier, S.; Baird, M. C.; Kiss, G.; Roper, G. C.; Hoff, C. D. *J. Am. Chem. Soc.* **1992**, *114*, 907. (p) Goh, L. Y.; Habley, T. W.; Darensbourg, D. J.; Reibenspies, J. *J. Organomet. Chem.* **1990**, *381*, 349. (q) Guanyang, L.; Wing-Tak, W. *J. Organomet. Chem.* **1996**, *522*, 271. (r) Clegg, W.; Compton, N. A.; Errington, R. J.; Norman, N. C. *Acta Crystallogr.* **1988**, *C44*, 568. (s) Rheingold, A. L.; Harper, J. R. *Acta Crystallogr.* **1991**, *C47*, 184. (t) Richards, T. C.; Geiger, W. E.; Baird, M. C. *Organometallics* **1994**, *13*, 4494. (u) Woska, D. C.; Ni, Y.; Wayland, B. B. *Inorg. Chem.* **1999**, *38*, 4135. (v) O'Callaghan, K. A. E.; Brown, S. J.; Page, J. A.; Baird, M. C.; Richards, T. C.; Geiger, W. E. *Organometallics* **1991**, *10*, 3119. (w) Yao, Q.; Bakac, A.; Espenson, J. H. *Organometallics* **1993**, *12*, 2010. (x) Kadish, K. M.; Lacombe, D. A.; Anderson, J. E. *Inorg. Chem.* **1986**, *25*, 2246. The potentials in this paper have been converted to the ferrocene reference potential by addition of 0.46 V. (y) Morton, J. R.; Preston, K. F.; Cooley, N. A.; Baird, M. C.; Krusic, P. J.; McLain, S. J. *J. Chem. Soc., Faraday Trans. 1* **1987**, *83*, 3535.

(4) Cashman, D.; Lalor, F. J. *J. Organomet. Chem.* **1971**, *32*, 351.

(5) For reviews see: (a) Baird, M. C. *Organomet. Radical Processes* **1990**, 49. (b) Baird, M. C. *Chem. Rev.* **1988**, *88*, 1217.

(6) (a) Pickett, C. J.; Pletcher, D. *J. Chem. Soc., Dalton Trans.* **1975**, 879. (b) Chum, H. L.; Koran, D.; Osteryoung, R. A. *J. Organomet. Chem.* **1977**, *140*, 349. (c) Bagchi, R. N.; Bond, A. M.; Colton, R.; Luscombe, D. L.; Moir, J. E. *J. Am. Chem. Soc.* **1986**, *108*, 3352.

(7) (a) Bond, A. M.; Colton, R.; Kevekordes, J. E.; Panagiotidou, P. *Inorg. Chem.* **1987**, *26*, 1430. (b) Bond, A. M.; Colton, R.; Kevekordes, J. E. *Inorg. Chem.* **1987**, *25*, 749. (c) Bagchi, R. N.; Bond, A. M.; Brian, G.; Colton, R.; Henderson, T. L. E.; Kevekordes, J. E *Organometallics* **1984**, *3*, 4. (d) Bond, A. M.; Carr, S. W.; Colton, R. *Inorg. Chem.* **1984**, *23*, 2343. (e) Bond, A. M.; Carr, S. W.; Colton, R. *Organometallics* **1984**, *3*, 541. (f) Lappert, M. F.; McCabe, R. W.; MacQuitty, J. J.; Pye, P. L.; Riley, P. I. *J. Chem. Soc., Dalton Trans.* **1980**, 90. (g) Ashford, P. K.; Baker, P. K.; Connelly, N. G.; Kelly, R. L.; Woodley, V. A. *J. Chem. Soc., Dalton Trans.* **1982**, 477.

(8) (a) Connelly, N. G.; Demidowicz, Z.; Kelly, R. L. *J. Chem Soc., Dalton Trans.* **1975**, 2335. (b) Van Order, N.; Geiger, W. E.; Bitterwolf, T. E.; Rheingold, A. L. *J. Am. Chem. Soc.* **1987**, *109*, 5680. (c) Doxsee, K. M.; Grubbs, R. H.; Anson, F. C. *J. Am. Chem. Soc.* **1984**, *106*, 7819. (d) Zoski, C. G.; Sweigart, D. A.; Stone, N. J.; Rieger, P. H.; Mocellin, E.; Mann, T. F.; Mann, D. R.; Gosser, D. K.; Doeff, M. M.; Bond, A. M. *J. Am. Chem. Soc.* **1988**, *110*, 2109. (e) Camire, N.; Nafady, A.; Geiger, W. E. *J. Am. Chem. Soc.* **2002**, *124*, 7260.

(9) Shaw, M. J.; Geiger, W. E. *Organometallics* **1996**, *15*, 13.

(10) Nafady, A.; Chin, T. T.; Geiger, W. E. *Organometallics* **2006**, *25*, 1654, and references therein.

with $K[B(C_6F_5)_4]$ (Boulder Scientific Co.) in methanol,[11] recrystallized three times from CH_2Cl_2/ether, and dried at 353 K under vacuum for 20 h.

Spectroelectrochemical IR experiments were performed using Schlenk conditions under an atmosphere of argon after adding solvent and electrolyte to the electrochemical cell in a Vacuum Atmospheres drybox under nitrogen. All other experiments were conducted directly in the drybox under nitrogen. Working electrodes were glassy carbon electrodes (GCEs, 1−3 mm diameter) supplied by Bioanalytical Systems. The effective areas of the electrodes were determined through chronoamperometric measurements of ferrocene in acetonitrile/0.1 M $[NBu_4][PF_6]$. The electrodes were pretreated by polishing with successively finer diamond paste (Buehler, 3 to 0.25 μm) interspersed by washings with Nanopure water and, finally, dried in the antechamber of the drybox. Controlled potential coulometry was carried out using a basket-shaped Pt mesh electrode. Although the functional reference electrode was Ag/AgCl, separated from the working compartment by a fine glass frit, all potentials reported in this paper are versus the $FeCp_2^{0/+}$ redox couple, as recommended elsewhere.[12] The ferrocene potential was obtained by adding it to the solution at an appropriate point in the experiment. The supporting electrolyte in all experiments was $[NBu_4][B(C_6F_5)_4]$,[12,13] at concentrations of 0.05 or 0.1 M, as noted in the text. Diagnostics applied to the shapes and positions of cyclic voltammetric waves were as described earlier.[14] Digital simulations of background-subtracted cyclic voltammetry experiments were performed using Digisim 3.0 (Bioanalytical Systems). More details on the electrochemical methodologies can be found in a recent paper.[15]

X-ray crystal structure determinations were performed in the X-ray Crystallography Laboratory at Queen's University. Crystals were mounted on glass fibers with epoxy glue, and data collections were performed on a Bruker Smart CCD 1000 X-ray diffractometer with graphite-monochromated Mo Kα radiation (λ = 0.71073 Å) controlled with a Crysostream Controller 700. No significant decay was observed during data collections. Data were processed on a PC using the Bruker AXS Crystal Structure Analysis Package. Data collection: APEX2 (Bruker, 2006); cell refinement: SAINT (Bruker, 2005); data reduction: SAINT (Bruker, 2005); structure solution: XPREP (Bruker, 2005) and SHELXTL (Bruker, 2000); structure refinement: SHELXTL; molecular graphics: SHELXTL; publication materials: SHELXTL.[16a] Neutral atom scattering factors were taken from Cromer and Waber.[16b] The raw intensity data were converted (including corrections for scan speed, background and Lorentz and polarization effects) to structure amplitudes and their esd's using the program SAINT, which corrects for *Lp* and decay. Absorption corrections were applied using the program SADABS. All non-hydrogen atoms were refined anisotropically. The positions for all hydrogen atoms were calculated (unless otherwise stated), and their contributions were included in the structure factors and calculations.

Table 1. Selected Bond Lengths and Angles of $[\mathbf{1_2}][B(C_6F_5)_4]_2$, $[\mathbf{2_2}][B(C_6F_5)_4]_2$, and $[\mathbf{3_2}][B(C_6F_5)_4]_2$

	$[\mathbf{1_2}][B(C_6F_5)_4]_2$	$[\mathbf{2_2}][B(C_6F_5)_4]_2$	$[\mathbf{3_2}][B(C_6F_5)_4]_2$
Bond Lengths (Å)			
P(1)−C(1)	1.784(2)	1.777(8)	1.777(5)
P−Me	1.792(2)	1.782(9)	1.789(5)
P−Ph av	1.788	1.776	1.794
M−C_5 centroid	1.847	2.010	2.001
C(1)−C(2)	1.428(3)	1.447(12)	1.451(7)
C(1)−C(5)	1.425(3)	1.440(12)	1.445(7)
C(2)−C(3)	1.410(3)	1.399(13)	1.419(7)
C(4)−C(5)	1.411(3)	1.435(12)	1.397(7)
C(3)−C(4)	1.406(4)	1.390(15)	1.418(8)
C(1)−metal	2.164(2)	2.305(8)	2.298(5)
C(2)−metal	2.197(2)	2.319(9)	2.342(5)
C(3)−metal	2.253(2)	2.355(9)	2.388(5)
C(4)−metal	2.230(2)	2.411(8)	2.367(5)
C(5)−metal	2.178(2)	2.337(8)	2.304(5)
Bond Angles (deg)			
C(1)−P−Me	108.92(11)	107.7(5)	108.3(2)
C(1)−P−Ph av	108.9	109.8	109.5
Me−P−Ph av	110.1	109.2	110
Ph−P−Ph	109.66(11)	110.8(4)	109.6(2)
P−C(1)−C_5 centroid	173.2	172.0	172.9
C(1)−C(2)−C(3)	107.7(2)	106.6(9)	107.2(4)
C(2)−C(3)−C(4)	108.8(2)	112.1(9)	109.3(5)
C(3)−C(4)−C(5)	108.0(2)	106.1(8)	108.0(5)
C(4)−C(5)−C(1)	108.3(2)	108.7(9)	109.1(5)
C(5)−C(1)−C(2)	107.2(2)	106.6(7)	106.4(4)

In the case of $[\mathbf{1_2}][B(C_6F_5)_4]_2$, the hydrogen atoms on one of the dichloromethane molecules were located from the difference Fourier map, but all of the other hydrogen atoms were calculated and their contributions were included in the structure factor calculations. For $[\mathbf{2_2}]$, the positions of all non-hydrogen atoms were refined anisotropically. The positions for all hydrogen atoms were calculated and their contributions were included in the structure factor calculations. However, the structure can only be refined to R1 ≈ 13% with a THF molecule disordered. ROTAX[16c] was thus used to find the twin law. The twin law [1 0 0 0 −1 0 −0.252 0 −1] of merit (fom) 2.48 for 180° rotation was applied to the refinement and the R1 dropped to ∼10%. The crystal was thus considered to be merohedrally twinned. SQEEZE[16d] was then applied to squeeze out the 1.5 THF molecule, which led to R1 ≈ 8.8%. For $[\mathbf{3_2}][B(C_6F_5)_4]_2$, the disordered THF solvent molecule was refined with DFIX, EADP, and PART. Selected bond lengths and angles for all three dimers are provided in Table 1, general crystallographic data in Table 2, and comparisons of metal−metal bond distances with those of the η^5-C_5H_5 and η^5-C_5Me_5 analogues in Table 3.

Synthesis of $[Cr(\eta^5\text{-}C_5H_4PMePh_2)(CO)_3]_2[B(C_6F_5)_4]_2$, $[\mathbf{1_2}][B(C_6F_5)_4]_2$. A solution of 0.110 g of **1** (1.3×10^{-4} mol) and 0.051 g of $[FeCp_2][B(C_6F_5)_4]$ (1.3×10^{-4} mol) in 5 mL of CH_2Cl_2 was stirred for 30 min, during which time it changed from deep green to yellow-brown. The solution was then layered with 30 mL of hexanes and cooled to −30 °C to give green crystals, which were filtered and washed with 3 × 20 mL of hexanes. Yield: 0.104 g (76%). Anal. Found: C 46.90, H 1.57. Calc for $C_{90}H_{34}B_2F_{40}P_2O_6Cr_2 \cdot 3CH_2Cl_2$: 47.45, H 1.64. IR data are given in Table 4. ^{1}H NMR (CD_2Cl_2, 298 K, 600 MHz): δ 28.80 (2H, br s, C_5H_4), 13.65 (2H, br s, C_5H_4), 7.85−7.60 (10H, br, *Ph*), 1.18 (3H, br, *Me*). ^{1}H NMR (THF-d_8, 298 K, 600 MHz): δ 26.08 (2H, br, C_5H_4), 13.62 (2H, br, C_5H_4), 8.07−7.66 (10H, *Ph*), 2.34 (3 H, br s, *Me*). ^{1}H NMR (THF-d_8, 213 K, 600 MHz): δ 7.95−7.75 (10H, m, *Ph*), 6.12 (1H, br, C_5H_4), 5.96 (1H, br, C_5H_4), 5.85 (1H, br, C_5H_4), 5.65 (1H, br, C_5H_4), 2.89 (3H, br, *Me*). HR ES-MS (THF): found 400.0320 *m*/*z*; calc 400.0348 (diff 6.8926 ppm). MS−MS experiments showed that the peak at 400 *m*/*z* (target ion) was responsible for the fragment at 316 *m*/*z* (loss of 84 amu = loss of 3CO).

(11) LeSuer, R. J.; Buttolph, C.; Geiger, W. E. *Anal. Chem.* **2004**, *76*, 6395.

(12) (a) Gritzner, G.; Kuta, J. *Pure Appl. Chem.* **1984**, *56*, 461. (b) Connelly, N. G.; Geiger, W. E. *Chem. Rev.* **1996**, *96*, 877.

(13) LeSuer, R. J.; Geiger, W. E. *Angew. Chem., Int. Ed.* **2000**, *39*, 248.

(14) Geiger, W. E. In *Laboratory Methods in Electroanalytical Chemistry*, 2nd ed.; Kissinger, P. T., Heineman, W. E., Eds.; Marcel Dekker, Inc.; New York, 1996; Chapter 23.

(15) Nafady, A.; Costa, P. J.; Calhorda, M. J.; Geiger, W. E. *J. Am. Chem. Soc.* **2006**, *128*, 16587.

(16) (a) *Bruker AXS*, Crystal Structure Analysis Package; Bruker, 2000. *SHELXTL*, Version 6.14; Bruker AXS Inc.: Madison, WI, 2005. *XPREP*, Version 2005/2; Bruker AXS Inc.: Madison, WI, 2005. *SAINT*, Version 7.23A; Bruker AXS Inc.: Madison, WI, 2006. *APEX2*, Version 2.0-2; Bruker AXS Inc.: Madison, WI. (b) Cromer, D. T.; Waber, J. T. *International Tables for X-ray Crystallography*; Kynoch Press: Birmingham, UK, 1974; Vol. 4, Table 2.2 A. (c) Cooper, R. I., Gould, R. O., Parsons, S.; Watkin, D. J. *J. Appl. Crystallogr.* **2002**, *35*, 168. (d) Sluis, P. v. d.; Spek, A. L. *Acta Crystallogr.* **1990**, *A46*, 194.

Table 2. Crystallographic Data

	$[\mathbf{1}_2][B(C_6F_5)_4]_2$	$[\mathbf{2}_2][B(C_6F_5)_4]_2$	$[\mathbf{3}_2][B(C_6F_5)_4]_2$
empirical formula, fw	$C_{93}H_{40}B_2Cl_6Cr_2F_{40}O_6P_2$, 2413.51	$C102H_{58}B_2F_{40}Mo_2O_9P_2$, 2462.92	$C_{102}H_{58}B_2F_{40}O_9P_2W_2$, 2638.74
temperature (K)	180(2)	298(2)	180(2)
wavelength (Å)	0.71073	0.71073	0.71073
cryst syst	triclinic	monoclinic	monoclinic
space group	$P\bar{1}$	$P2/n$	$P2/n$
a (Å)	9.8319(4)	13.0003(18)	12.9575(7)
b (Å)	12.8275(6)	10.0517(14)	9.9157(6)
c (Å)	19.6330(9)	38.132(5)	37.847(2)
α (deg)	70.9350(10)	90	90
β (deg)	83.1200(10)	92.466(2)	91.9600(10)
γ (deg)	88.6700(10)	90	90
V (Å^3)	2323.09(18)	4978.3(12)	4859.8(5) Å^3
Z	1	2	2
ρ (calcd) (Mg/m^3)	1.725	1.643	1.803
absorp coeff (mm^{-1})	0.577	0.418	2.535
F(000)	1196	2452	2580
cryst size (mm^3)	0.15 × 0.15 × 0.10	0.25 × 0.20 × 0.06	0.15 × 0.12 × 0.10
θ range for data collection (deg)	2.09 to 25.00	2.03 to 25.19	1.68 to 25.00
index ranges	$-11\le h\le 11$, $-15\le k\le 15$, $-23\le l\le 23$	$-15\le h\le 15$, $-12\le k\le 12$, $-45\le l\le 45$	$-15\le h\le 15$, $-11\le k\le 11$, $-44\le l\le 44$
no. of reflns collected	16 270	44 366	44 056
no. of indep reflns	8129 [R(int) = 0.0191]	8919 [R(int) = 0.0840]	8569 [R(int) = 0.0418]
completeness to θ = 25.00°	99.30%	99.50%	99.90%
absorp corr	multiscan	numerical	multiscan
max. and min. transmn	0.9445 and 0.9184	0.9754 and 0.9028	0.7856 and 0.7023
refinement method	full-matrix least-squares on F^2	full-matrix least-squares on F^2	full-matrix least-squares on F^2
no. of data/restraints/ params	8129/2/738	8919/0/641	8569/4/729
goodness-of-fit on F^2	1.00	1.054	1.00
final R indices [$I > 2\sigma(I)$]	R1 = 0.0351, wR2 = 0.0940	R1 = 0.0881, wR2 = 0.2110	R1 = 0.0376, wR2 = 0.1283
R indices (all data)	R1 = 0.0467, wR2 = 0.1023	R1 = 0.1209, wR2 = 0.2248	R1 = 0.0453, wR2 = 0.1369
largest diff peak and hole (e Å^{-3})	0.352 and −0.449	1.192 and −0.928	0.852 and −1.104

Table 3. Comparison of Metal−Metal Bond Distances of $[M(\eta^5\text{-}C_5H_5)(CO)_3]_2$, $[M(\eta^5\text{-}C_5Me_5)(CO)_3]_2$, and $[M(\eta^5\text{-}C_5H_4PMePh_2)(CO)_3]_2[B(C_6F_5)_4]_2$ (M = Cr, Mo, W)

metal	$[M(\eta^5\text{-}C_5H_5)(CO)_3]_2$	$[M(\eta^5\text{-}C_5Me_5)(CO)_3]_2$	$[M(\eta^5\text{-}C_5H_4PMePh_2)(CO)_3]_2^{2+}$
Cr	3.281(1)[3a]	3.311(1),[3o] 3.310(1)[3p]	3.3509(7)
Mo	3.235(1)[3a]	3.284(1),[3q] 3.281(1)[3r]	3.2764(16)
W	3.222(1)[3a]	3.288(1)[3s]	3.2507(4)

Table 4. Solution (THF) and Solid-State (Fluorolube mulls) IR Data (ν(CO)) of $[M(\eta^5\text{-}C_5H_4PMePh_2)(CO)_3]_2[B(C_6F_5)_4]_2$ (M = Cr, Mo, W)

metal	THF (cm^{-1})	CH_2Cl_2 (cm^{-1})	Fluorolube (cm^{-1})
Cr	2037 (s), 1955 (s br), 1914 (s br)	2035, 1955, 1910	2036 (vw), 1970, 1949, 1932, 1897 (w sh)
Mo	2025 (w), 1976 (s br), 1939 (s br), ∼1922 (sh)	2029, 1981, 1943	2037 (vw), 1975, 1939, 1932
W	2023 (w), 1973 (s br), 1933 (s br), ∼1922 (sh)		1972, 1925

Synthesis of $[Mo(\eta^5\text{-}C_5H_4PMePh_2)(CO)_3]_2[B(C_6F_5)_4]_2$, $[\mathbf{2}_2][B(C_6F_5)_4]_2$. In a procedure similar to that described above, a solution of 0.096 g of **2** (2.2 × 10^{-4} mol) and 0.186 g of $[FeCp_2][B(C_6F_5)_4]$ (2.2 × 10^{-4} mol) in 10 mL of THF was stirred for 30 min, turning from reddish-green to red. The resulting solution was layered with 30 mL of hexanes and cooled to −30 °C to yield a red oil, which slowly solidified. The oil was washed with 3 × 15 mL of hexanes and dried *in vacuo* to give a red solid in a yield of 0.207 g (86%). X-ray quality crystals were grown from a solution of the red material in a 1:4 mixture of CH_2Cl_2/THF layered with hexanes and kept at −30 °C. Anal, Found: C 47.30, H 1.67. Calc for $C_{90}H_{34}B_2F_{40}P_2O_6Mo_2$: 48.12, H 1.53. IR data are given in Table 4. ^{1}H NMR (THF-d_8, 298 K, 600 MHz): δ 7.87−7.72 (10 H, m, *Ph*), 6.10−6.04 (2H, br m, C_5H_4) and 5.91 (2H, br m, C_5H_4), 2.88 (3H, d, *Me*, $^2J_{P-H}$ 11.0 Hz). ^{31}P NMR (THF-d_8, 121 MHz): δ 19.88. ^{13}C NMR (THF-d_8, 150 MHz): δ 231.5 (*C*O), 224.8 (*C*O), 149.4 (m, *o*-C_6F_5), 139.4 (m, *p*-C_6F_5), 138.3 (m, *m*-C_6F_5), 136.7 (br s, *p*-Ph), 133.7 (d, J_{P-C} 11.0 Hz, Ph), 131.5 (d, J_{P-C} 13.2 Hz, Ph), 125.6 (br m, *ipso*-C_6F_5), 121.7 (d, J_{P-C} 90.0 Hz, *ipso*-Ph), 103.0 (d, J_{P-C} 8.8 Hz, PC*C*HCH), 97.2 (d, J_{P-C} 11.0 Hz, PCCH*C*H), 86.1 (d, J_{P-C} 94.4 Hz, P*C*CHCH), 8.4 (d, J_{P-C} 60.4 Hz, Me). HR ES-MS (THF): found 445.9969 *m*/*z*; calc 445.9988 (diff 4.1748 ppm).

Synthesis of $[W(\eta^5\text{-}C_5H_4PMePh_2)(CO)_3]_2[B(C_6F_5)_4]_2$, $[\mathbf{3}_2][B(C_6F_5)_4]_2$. A solution of 0.088 g of **3** (1.7 × 10^{-4} mol) and 0.143 g of $[FeCp_2][B(C_6F_5)_4]$ (1.7 × 10^{-4} mol) in 10 mL of THF was stirred for 30 min. The resulting solution was layered with 30 mL of hexanes and cooled to −30 °C to yield a red oil, which slowly solidified. The oil was washed with 3 × 15 mL of hexanes and dried *in vacuo* to give a red solid in a yield of 0.155 g (77%). X-ray quality crystals were grown from a dilute THF solution (∼20 mg in 1.5 mL of THF) layered with hexanes and kept at room temperature. Anal. Found: C 44.67, H 1.94. Calc for $C_{90}H_{34}B_2F_{40}P_2O_6W_2$: 44.62, H 1.41. IR data are given in Table 4. ^{1}H NMR (THF-d_8, 298 K, 600 MHz): δ 7.80−7.71 (10H m, *Ph*), 6.05 (4H, br m, C_5H_4), 2.86 (3H, br d, $^2J_{P-H}$ 12.8 Hz, Me). ^{13}C NMR (THF-d_8, 150 MHz): δ 218.5 (s, *C*O), 211.7 (s, *C*O), 149.4 (m, *o*-C_6F_5), 139.4 (m, *p*-C_6F_5), 137.3 (m, *m*-C_6F_5), 136.8 (d, J_{P-C} 2.8 Hz, *p*-Ph), 133.8 (d, J_{P-C} 12.5 Hz, Ph), 131.5 (d, J_{P-C} 13.9 Hz, Ph), 125.6 (br m, *ipso*-C_6F_5), 121.4 (d, J_{P-C} 90.2 Hz, *ipso*-Ph), 102.8

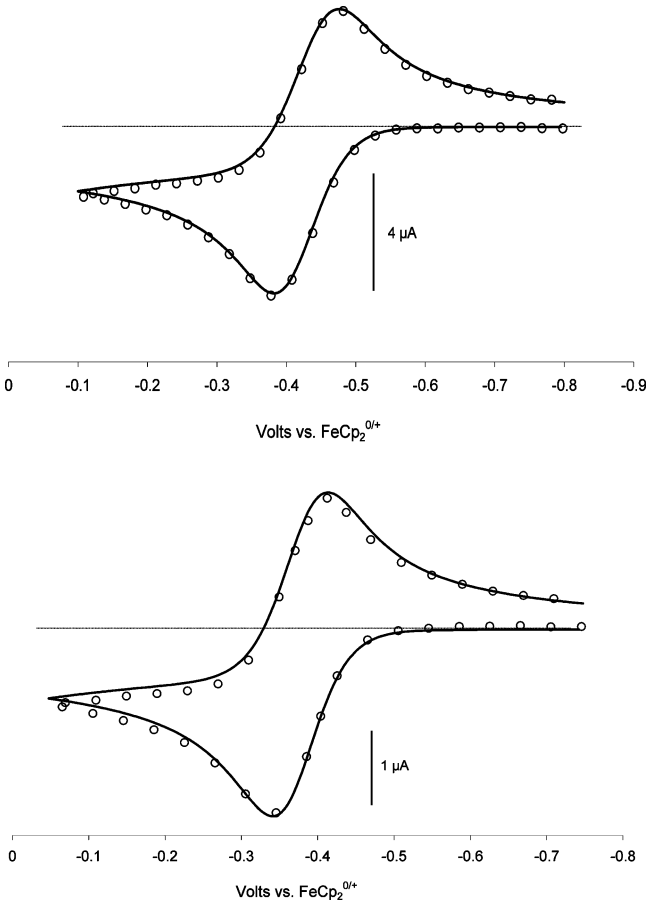

Figure 1. Experimental (circles) and simulated CVs for 0.6 mM **1** in CH_2Cl_2/0.1 M $[NBu_4][B(C_6F_5)_4]$. Top, $v = 2.0$ V s^{-1}; bottom, $v = 0.3$ V s^{-1}. Relevant simulation parameters: $k_s = 0.04$ cm s^{-1}, $\beta = 0.57$.

(d, J_{P-C} 8.3 Hz, PC*C*HCH), 94.4 (d, J_{P-C} 11.1 Hz, PCCH*C*H), 84.3 (d, J_{P-C} 97.1 Hz, P*C*CHCH), 8.4 (d, J_{P-C} 59.6 Hz, Me). ^{31}P NMR (THF-d_8, 121 MHz): δ 20.76. HR ES-MS(THF): found 532.0424 *m/z*; calc 532.0406 (diff 3.5448 ppm).

Oxidation of 1 with $[Ph_3C][B(C_6F_5)_4]$. A solution of 0.400 g of **1** (9.99×10^{-4} mol) and 0.968 g of $[Ph_3C][B(C_6F_5)_4]$ (1.05×10^{-3} mol) in 15 mL of THF was stirred for 30 min, the green solution slowly turning yellow. The solution was then layered with ~100 mL of hexanes and cooled to −30 °C, and a green solid precipitated and was separated from the supernatant. The solid was washed with 4 × 10 mL of hexanes before being dried *in vacuo* to yield 0.917 g (85%) of $[\mathbf{1}_2][B(C_6F_5)_4]_2$. This material had an IR spectrum identical to that of the material prepared using $[FeCp_2][B(C_6F_5)_4]$ as oxidant.

Oxidation of 1 with $[FeCp_2][PF_6]$. A solution of 0.130 g of **1** (3.25×10^{-4} mol) and 0.108 g of $[FeCp_2][PF_6]$ (3.25×10^{-4} mol) in 10 mL of THF was stirred for 1.5 h, turning to a deep brownish-yellow-green color. As the reaction proceeded, it was monitored by IR spectroscopy, which showed the growth of peaks at 2030, 1941, and 1906 cm^{-1}, identical to those of the $[\mathbf{1}_2][B(C_6F_5)_4]_2$ obtained using $[FeCp_2][B(C_6F_5)_4]$, and a new set of peaks (already present after 5 min) at 1917, 1821, and 1808 cm^{-1}.

Results and Discussion

Electrochemical Oxidation of 1, 2, and 3. Cyclic voltammograms (CVs) of **1** in CH_2Cl_2 with 0.05 M $[NBu_4][B(C_6F_5)_4]$ exhibited an oxidation wave at $E_{1/2} = -0.38$ V (Figure 1) having the general characteristics of a chemically reversible one-electron process as given in eq 1. This conclusion was confirmed by bulk coulometry (see below).

$$Cr(\eta^5\text{-}C_5H_4PMePh_2)(CO)_3\ (\mathbf{1}) - e^- \rightleftharpoons [Cr(\eta^5\text{-}C_5H_4PMePh_2)(CO)_3]^+\ (\mathbf{1}^+) \quad (1)$$

A second, chemically irreversible anodic wave of approximately one-half of the height of the first wave was observed at E_{pa} = ca. 0.95 V (Figure SM1, Supporting Information), but the products of this second oxidation were not studied. The free cyclopentadienylide ligand itself oxidizes (irreversibly) at $E_{pa} = 0.1$ V. Owing to the fact that, as will be shown, the molybdenum and tungsten analogues **2** and **3** undergo fast dimerization reactions when oxidized, the oxidation of **1** was also investigated under conditions, specifically at lower temperatures and higher concentrations, that would be expected to favor dimerization of $\mathbf{1}^+$. CV scans of a 3.6 mM solution of **1** in CH_2Cl_2 at temperatures from ambient to 238 K failed to show any changes that would indicate involvement of dimerization of $\mathbf{1}^+$ in detectable amounts in solution. Simulations of CV scans of **1** (Figure 1) provide values of the charge-transfer coefficient, $\beta = 0.57$ (where $\beta = 1 - \alpha$), and the standard heterogeneous electron-transfer rate constant, $k_s = 0.04$ cm s^{-1}, for the reversible one-electron oxidation. The diffusion coefficient of **1** was measured as $D_o = 5 \times 10^{-6}$ cm^2 s^{-1}.

Bulk electrolysis of **1** at $E_{appl} = 0.3$ V resulted in clean conversion to the radical cation $\mathbf{1}^+$ as the color of the solution remained yellow. The coulometry was consistent with a one-electron process, with values of 0.90 and 0.95 F/equiv being obtained in two separate experiments. The starting material **1** was efficiently regenerated to greater than 90% of its original concentration by back-electrolysis at $E_{appl} = -0.6$ V. When monitored by *in situ* IR spectroscopy (Figure 2), the anodic electrolysis revealed the presence of three carbonyl bands for the 17-electron species $\mathbf{1}^+$, at 2035, 1955, and 1910 cm^{-1}, comparable with the values of ν_{CO} of $[\mathbf{1}_2^{2+}][B(C_6F_5)_4]_2$ prepared from the oxidation of **1** by $[FeCp_2][B(C_6F_5)_4]$ (see below) and at considerably higher frequencies than ν_{CO} of the neutral **1** (1912 and 1809 cm^{-1}).[1] Assuming that 1809 cm^{-1} may be taken as the average of the asymmetric ν_{CO} of **1**, an average shift of +124 cm^{-1} in ν_{CO} is calculated for the one-electron oxidation, in concert with expectations.[17] Taken together, the voltammetry, electrolysis, and IR spectroscopy indicate that the first oxidation of **1** is a quasi-Nernstian, chemically reversible, one-electron process involving a largely metal-based orbital; note that we have previously shown that the HOMO of **1** is indeed a metal-based orbital.[1] There is no evidence for appreciable amounts of the chromium dimer dication, $\mathbf{1}_2^{2+}$, under these conditions of temperature and concentration.

Cyclic voltammograms of **2** in CH_2Cl_2/0.05 M $[NBu_4][B(C_6F_5)_4]$ revealed two chemically irreversible features when the potential was scanned from −1.1 to +0.1 V (Figure 3). The anodic wave at $E_{pa} \approx -0.19$ V is due to the apparent one-electron oxidation of **2** to $\mathbf{2}^+$, and the cathodic feature at more negative potentials arises from a follow-up reaction of $\mathbf{2}^+$. Whereas the anodic wave has the shape of an electrochemi-

(17) Shifts of >100 cm^{-1} are widely observed for ν_{CO} when the positive charge on a metal carbonyl complex is increased by one (Nakamoto, K. *Infrared and Raman Spectra of Inorganic and Coordination Compounds*, 4th ed.; Wiley, New York, 1986; pp 292−293). For recent experimental and theoretical work showing that the origin of this effect is predominantly electrostatic, see: (a) Goldman, A. S.; Krogh-Jespersen, K. *J. Am. Chem. Soc.* **1996**, *118*, 12159. (b) Willner, H.; Aubke, F. *Angew. Chem., Int. Ed.* **1997**, *36*, 2402. (c) Ehlers, A. W., Ruiz-Morales, Y.; Baerends, E. J.; Ziegler, T. *Inorg. Chem.* **1997**, *36*, 5031.

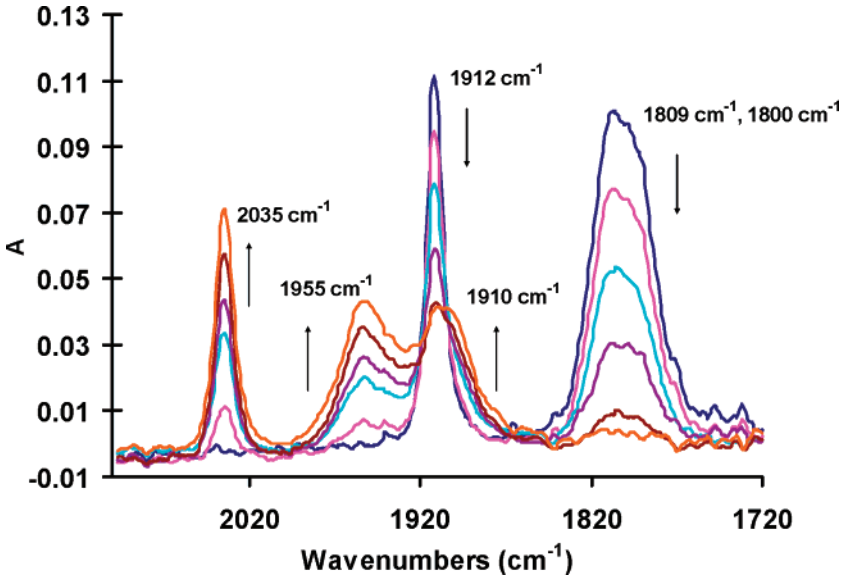

Figure 2. Infrared data for spectroelectrochemistry of 3.0 mM **1** in CH_2Cl_2/0.05 M $[NBu_4][B(C_6F_5)_4]$ at 298 K. Arrows indicate the increase or decrease in intensity of infrared absorptions as oxidation proceeds.

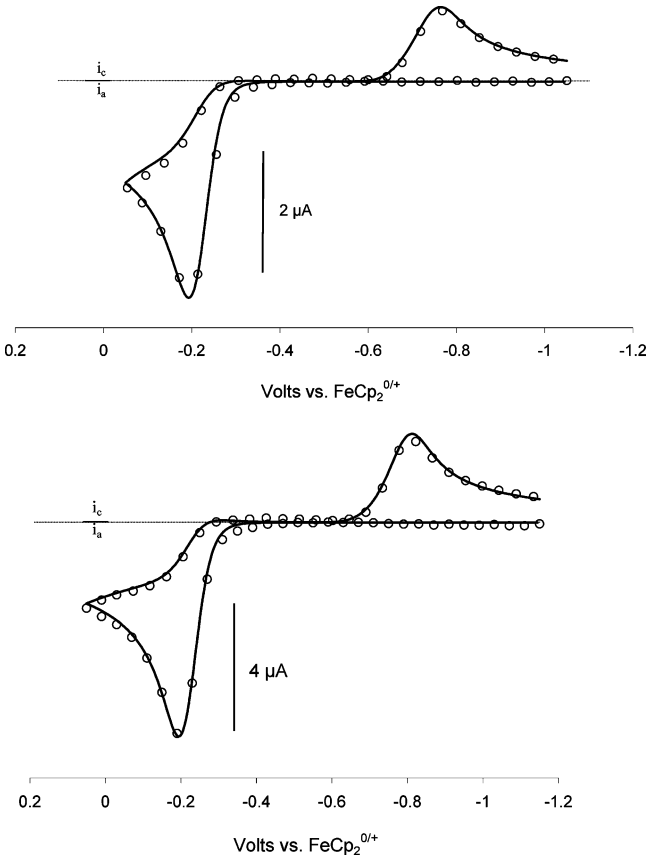

Figure 3. Experimental (circles) and simulated CVs for 0.7 mM **2** in CH_2Cl_2/0.1 M $[NBu_4][B(C_6F_5)_4]$. Top, $\upsilon = 0.5$ V s^{-1}; bottom, $\upsilon = 2.0$ V s^{-1}. Relevant simulation parameters: k_s (oxidation) = 0.1 cm s^{-1}, k_s (reduction) = 0.0025 cm s^{-1}, $K_{dim} = 1.0 \times 10^6$ M^{-1}, $k_f = 1.0 \times 10^6$ M^{-1} s^{-1}.

cally reversible process (i.e., one having relatively fast heterogeneous charge-transfer kinetics), the cathodic wave has the characteristics of an electrochemically irreversible process, being quite broad and exhibiting E_{pc} values that are highly scan rate dependent (e.g., −0.77 V at $\upsilon = 0.1$ V s^{-1} and −0.82 V at $\upsilon =$ 1 V s^{-1}).

Although there are a number of mechanisms that could account for these observations, the voltammetric behavior is most strongly reminiscent of an *anodic* EC mechanism, involving fast dimerization of $\mathbf{2}^+$ (eqs 2 and 3), and a *cathodic* two-electron EEC process resulting in regeneration of the original 18-electron complex **2** (eqs 4 and 5).

$$\text{Mo}(\eta^5\text{-C}_5\text{H}_4\text{PMePh}_2)(\text{CO})_3 - \text{e}^- \rightleftharpoons [\text{Mo}(\eta^5\text{-C}_5\text{H}_4\text{PMePh}_2)(\text{CO})_3]^+ \text{ (E)} \quad (2)$$

$$2[\text{Mo}(\eta^5\text{-C}_5\text{H}_4\text{PMePh}_2)(\text{CO})_3]^+ \rightleftharpoons [\text{Mo}(\eta^5\text{-C}_5\text{H}_4\text{PMePh}_2)(\text{CO})_3]_2^{2+} \text{ (C)} \quad (3)$$

$$[\text{Mo}(\eta^5\text{-C}_5\text{H}_4\text{PMePh}_2)(\text{CO})_3]_2^{2+} + 2\text{e}^- \rightarrow 2[\text{Mo}(\eta^5\text{-C}_5\text{H}_4\text{PMePh}_2)(\text{CO})_3]_2 \text{ (EE)} \quad (4)$$

$$[\text{Mo}(\eta^5\text{-C}_5\text{H}_4\text{PMePh}_2)(\text{CO})_3]_2 \rightarrow 2\text{Mo}(\eta^5\text{-C}_5\text{H}_4\text{PMePh}_2)(\text{CO})_3 \text{ (C)} \quad (5)$$

In the cathodic direction the "C" step (eq 5) involves homolytic cleavage of the Mo−Mo bond of the dimer. Since the data are insufficient to differentiate between the proposed EEC mechanism and an ECE cathodic mechanism in which fragmentation of the metal−metal bond occurs after the acceptance of the first electron, simulations were performed using only the EEC process for the cathodic reaction. There is significant literature precedent for these types of overall mechanisms in describing the redox-based formation and cleavage of metal−metal bonded organometallic dimers.[18] In the present case, the best fit to CV scans over the scan rate range of 0.5 to 2 V s^{-1} employed a dimerization equilibrium constant, K_{dim}, of 1×10^6 M^{-1} and a dimerization rate constant, k_{dim}, of 10^6 M^{-1} s^{-1}. It is clear from the cathodic wave shape that the charge-transfer coefficient, α, is less than 0.5 for the reduction process, and a good fit was obtained with $\alpha = 0.35$. Although the simulations agreed with experiment when the effective heterogeneous electron transfer was 0.0025 cm s^{-1},

(18) Chong, D. S.; Nafady, A.; Costa, P. J.; Calhorda, J. M.; Geiger, W. E. *J. Am. Chem. Soc.* **2005**, *127*, 15676, and references therein.

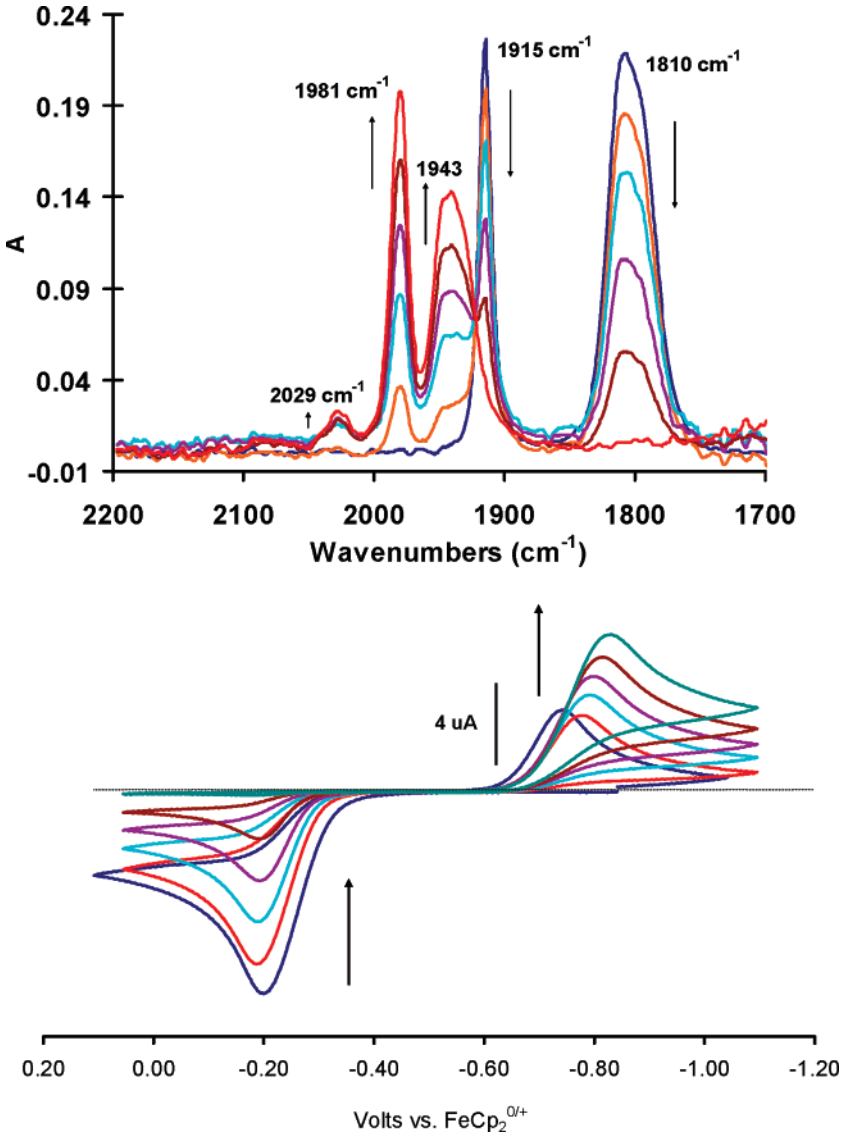

Figure 4. Spectroelectrochemical data for 3.0 mM **2** in CH_2Cl_2/0.05 M $[NBu_4][B(C_6F_5)_4]$ at 298 K. Arrows indicate the increase or decrease in signal intensity as oxidation proceeds. CVs taken at $\upsilon = 0.1$ V s^{-1}.

this value should be taken only as representative of a family of rate constants, α values, and $E_{1/2}$ values that would be consistent with the cathodic process.

When bulk anodic electrolysis of **2** was conducted at $E_{appl} = 0.15$ V, the pale yellow solution turned orange-pink as the red dimer dication, $\mathbf{2}_2^{2+}$, was formed. Voltammetry indicated essentially quantitative formation of $\mathbf{2}_2^{2+}$ as the single product, having an irreversible cathodic wave at E_{pc} of approximately −0.77 V, and back-reduction of this solution at $E_{appl} = -1.3$ V regenerated **2** in greater than 95% yield. One nuance of these experiments is that the coulometry count was consistently somewhat lower than that expected for a one-electron process, being 0.7 to 0.8 F/equiv in three separate electrolyses. *In situ* IR spectroscopy was therefore used to monitor the carbonyl region of the reactant and product. As shown in Figure 4, oxidation resulted in disappearance of the symmetric and asymmetric ν_{CO} of **2** at 1915 and 1810 cm^{-1},[1] respectively, and the appearance of at least three new terminal carbonyl bands, at 2029, 1981, and 1943 cm^{-1} and very close to the ν(CO) of $[Mo(\eta^5\text{-}C_5H_4PMePh_2)(CO)_3]_2[B(C_6F_5)_4]_2$ in THF (Table 4). The fact that there is an isosbestic point at 1920 cm^{-1} demonstrates that the new absorption bands arise from a single product, the dimer dication $\mathbf{2}_2^{2+}$.

The cyclic voltammetric characteristics of **3** in CH_2Cl_2/0.05 M $[NBu_4][B(C_6F_5)_4]$ were very similar to those of the molybdenum analogue, with only slight shifts in potential being noted.[19] At a scan rate of 0.1 V s^{-1}, the chemically irreversible oxidation peak appeared at $E_{pa} = -0.20$ V and the irreversible cathodic product peak was found at $E_{pc} = -0.81$ V. More detailed work on this system was not pursued, owing to its apparent mechanistic similarity to **2**.

As shown previously,[1] methyldiphenylphosphonium cyclopentadienylide is less electron donating than is the formally anionic η^5-cyclopentadienyl ligand. This accounts for the fact that compounds **1**−**3** oxidize at potentials that are considerably more positive than do their 18-electron analogues, $[M(\eta^5\text{-}C_5H_5)(CO)_3]^-$, for which $E_{1/2}$ values of −0.82,[3t] −0.75,[3x] and −0.85 V[3x] were observed for the chromium, molybdenum, and tungsten complexes, respectively. The $[PMePh_2]^+$ group therefore stabilizes this family of 18-electron complexes against one-electron oxidation by 440−650 mV. The ligand electronic effect must be taken from the shift of 440 mV observed for the reversible processes of the Cr complexes. In the context of other acceptor

(19) For both compounds **2** and **3**, a second irreversible anodic wave is observed at approximately $E_{pa} = 1.40$ V, apparently due to the oxidation of the respective dimer dications formed near the electrode surface.

Scheme 1. Synthetic Route to the Complexes $[M(\eta^5\text{-}C_5H_4PMePh_2)(CO)_3]_2[B(C_6F_5)_4]_2$ (M = Cr, Mo, W)

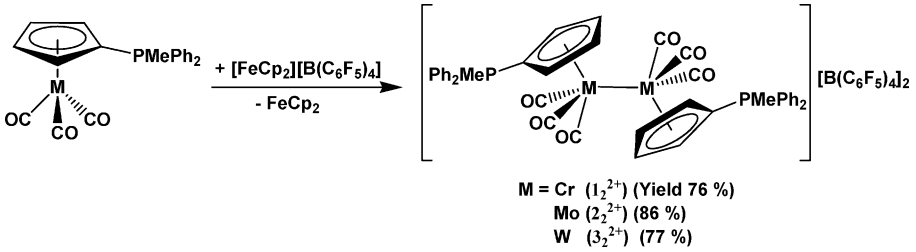

M = Cr (1_2^{2+}) (Yield 76 %)
Mo (2_2^{2+}) (86 %)
W (3_2^{2+}) (77 %)

substituents, this group has a greater electronic effect than a bromine atom, an aldehyde group, or a trifluoromethyl group (shifts of 170, 280, and 320 mV, respectively) and about the same effect as the strongly electron-withdrawing perfluorophosphazine group, $N_3P_3F_5$.[20,2l] Put another way, the $[PMePh_2]^+$ group is at least as electron withdrawing as an amino group is electron donating, evidenced by the fact that the NH_2 substituent effect on a C_5H_4R ring is only −370 mV.[21,22] The electrostatic effect of the phosphonium moiety is undoubtedly the major reason for this result.

Bulk Syntheses of $[M(\eta^5\text{-}C_5H_4PMePh_2)(CO)_3]_2[B(C_6F_5)_4]_2$ (M = Cr, Mo and W). The syntheses of $[M(\eta^5\text{-}C_5H_4PMePh_2)(CO)_3]_2[B(C_6F_5)_4]_2$ (M = Cr, Mo and W) were carried out in CH_2Cl_2 (Cr) or THF (Mo, W) by combining **1**, **2**, or **3** with equimolar amounts of ferrocenium tetrakisperfluorophenylborate, $[FeCp_2][B(C_6F_5)_4]$ (Scheme 1). Separation from ferrocene was readily achieved by recrystallizing the products from solutions of CH_2Cl_2 (M = Cr) or THF (M = Mo, W) by layering with hexanes. Although $\mathbf{1}^+$ is clearly the dominant species in the chromium system under these conditions, the electrolysis solution was ESR silent at room temperature, apparently a consequence of the fast relaxation phenomena often encountered with this family of metal-centered radicals.[3y] It is also important to note that the three complexes do not take part in chlorine atom abstraction reactions with CH_2Cl_2, which is a common concern when handling metal-centered radicals.[5]

Oxidation of **1** could also be effected using $[Ph_3C][B(C_6F_5)_4]$ since the trityl cation (Ph_3C^+) has a calculated reduction potential of $E_{1/2} \approx -0.12$ V versus $FeCp_2^{0/+}$.[23] The IR spectrum of the material formed was identical to that obtained using $[FeCp_2][B(C_6F_5)_4]$ and the yield was similar, and we note that the trityl ion has been used previously as an oxidant with the compound $Mo(\eta^5\text{-}C_5H_5)(CO)(dppe)H$ (dppe = $Ph_2PCH_2CH_2PPh_2$).[23] In contrast, while use of $[FeCp_2][PF_6]$ as an oxidant with **1** did result in the formation of the oxidized product $\mathbf{1}^+$ (IR), the formation of other products was evident even within the first 5 min of reaction. In addition to the ν(CO) observed for $\mathbf{1}^+$, peaks at 1917, 1821, and 1808 cm^{-1} were also observed and were the dominant features of the spectrum after 1.5 h. While the peaks at 1917 and 1808 cm^{-1} are identical to those of **1** in THF, we cannot propose a process that would result in the re-formation of **1**, and so these peaks are presumably to be attributed to an unknown product that has incorporated fluoride ion. Note that ν(CO) of $[(\eta^5\text{-}C_5H_4PMePh_2)Mo(CO)_3I]I$ are observed at 2055 and 1979 cm^{-1},[1] quite different from the ν(CO) observed here for the product of oxidation by $[FeCp_2][PF_6]$ and thus excluding an analogous fluoro complex.

X-ray Crystal Structures of $[M(\eta^5\text{-}C_5H_4PMePh_2)(CO)_3]_2[B(C_6F_5)_4]_2$ (M = Cr, Mo, and W). X-ray quality crystals of $[\mathbf{1_2}][B(C_6F_5)_4]_2$ were grown from a solution of CH_2Cl_2 layered with hexanes and kept at −30 °C; there are 1.5 CH_2Cl_2 molecules of solvation per mole of Cr in the unit cell, consistent with the elemental analyses. Initially crystals of the molybdenum and tungsten analogues were grown from 1:4 CH_2Cl_2/THF solutions layered with hexanes and kept at −30 °C, but twinned crystals were obtained in both cases. While the crystals of $[\mathbf{2_2}][B(C_6F_5)_4]_2$ were of sufficient quality for the structure to be solved with acceptable errors on bond lengths and angles, the twinned crystals of $[\mathbf{3_2}][B(C_6F_5)_4]_2$ did not yield acceptable crystallographic data. It was however possible to obtain untwinned X-ray quality crystals of the latter from a very dilute THF solution layered with hexanes and kept at room temperature over the course of three weeks. Crystals of the molybdenum and tungsten dimeric complexes each contain 1.5 THF molecules of solvation per mole of metal in the unit cell, but in these cases the solvent molecules were removed under reduced pressure prior to obtaining elemental analyses. The structures of $[\mathbf{1_2}][B(C_6F_5)_4]_2$ and $[\mathbf{3_2}][B(C_6F_5)_4]_2$ were solved by direct methods, but structural refinement of $[\mathbf{2_2}][B(C_6F_5)_4]_2$ required the use of ROTAX[16c] to find the twin law and then application of SQUEEZE[16d] to squeeze out the THF molecules of solvation.

The crystal structures of all three complexes show that the cations are present as dimers in the solid state. Selected bond lengths and angles are presented in Table 1, while crystallographic data are presented in Table 2, and the complete structures of $[\mathbf{1_2}][B(C_6F_5)_4]_2$ and $[\mathbf{2_2}][B(C_6F_5)_4]_2$ are presented in Figures 5 and 7, respectively; that of $[\mathbf{3_2}]^{2+}$, which is isomorphous with $[\mathbf{2_2}]^{2+}$, is not shown. For purposes of clarity, the structures of the cations, $[\mathbf{1_2}]^{2+}$ and $[\mathbf{2_2}]^{2+}$, with the anions deleted, are also shown in Figures 6 and 8. The Cr−Cr bond distance of the chromium complex is 3.3509(7) Å, apparently the longest Cr−Cr bond distance known for a compound not containing some type of bridging ligands. The longest Cr−Cr bond distance reported heretofore is 3.471(1) Å, observed in the bridged fulvalene (Fv) compound $[Cr_2(\mu\text{-Fv})(CO)_6]$, in which the geometry of the bridging ligand requires a long Cr−Cr bond.[24] The metal−metal bond of $[\mathbf{1_2}][B(C_6F_5)_4]_2$ is significantly longer than the Cr−Cr bonds in the analogous compounds $[Cr(\eta^5\text{-}C_5H_5)(CO)_3]_2$ (3.281(1) Å) and $[Cr(\eta^5\text{-}C_5Me_5)(CO)_3]_2$ (3.3107 (7) and 3.310(1) Å for two polymorphs); comparisons are shown in Table 3.[3a,o,p]

The metal−metal bond distances in $[\mathbf{2_2}][B(C_6F_5)_4]_2$ and $[\mathbf{3_2}][B(C_6F_5)_4]_2$ are 3.2764(16) and 3.2507(4) Å, respectively, shorter than the Cr−Cr bond of $[\mathbf{1_2}][B(C_6F_5)_4]_2$, as in the trend observed for the isoelectronic $\eta^5\text{-}C_5H_5$ and $\eta^5\text{-}C_5Me_5$ tricarbonyl deriva-

(20) Saraceno, R. A.; Riding, G. H.; Allcock, H. R.; Ewing, A. G. *J. Am. Chem. Soc.* **1988**, *110*, 980.

(21) For a compilation of substituent effects on the redox potentials of cyclopentadienyl complexes see: Lu, S.; Strelets, V. V.; Ryan, M. F.; Pietro, W. J.; Lever, A. B. P. *Inorg. Chem.* **1996**, *35*, 1013. Using the notation of this paper, the $[PMePh_2]^+$ group has an E_L(L) value of 0.77 V [the E_L(L) value of the cyclopentadienyl ligand is 0.33 V]. For reference to the $C_5H_4CF_3$ ligand see: Gassman, P. G.; Winter, C. H. *J. Am. Chem. Soc.* **1986**, *108*, 4228.

(22) Britton, W. E.; Kashyap, R.; El-Hashash, M.; El-Kady, M.; Herberhold, M. *Organometallics* **1986**, *5*, 1029.

(23) Cheng, T.-Y.; Szalda, D. J.; Zhang, J.; Bullock, R. M. *Inorg. Chem.* **2006**, *45*, 4712.

(24) McGovern, P. A.; Vollhardt, K. P. C. *Chem. Commun.* **1996**, 1593.

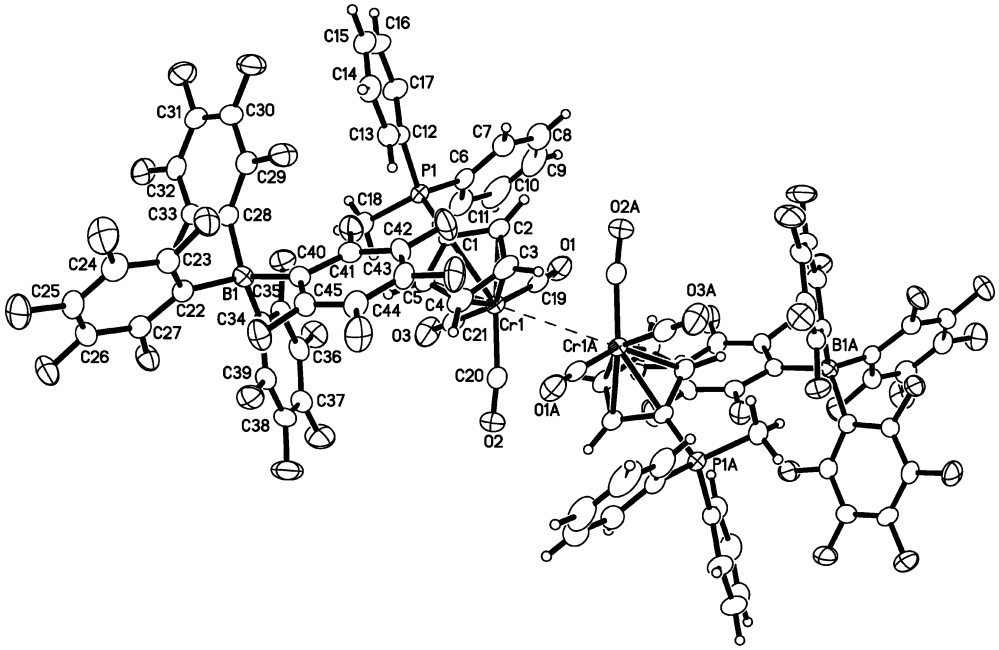

Figure 5. Complete molecular structure of $[\mathbf{1_2}][B(C_6F_5)_4]_2$.

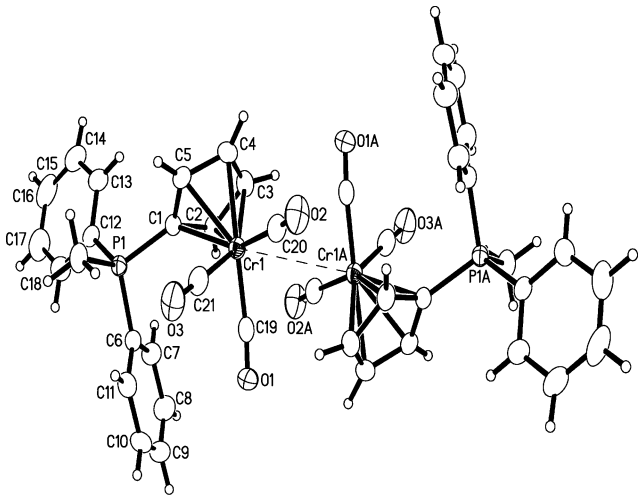

Figure 6. Structure of $[\mathbf{1_2}][B(C_6F_5)_4]_2$ with the anions omitted for clarity.

tives of chromium, molybdenum, and tungsten.[3] The complex $[\mathbf{2_2}][B(C_6F_5)_4]_2$ has a Mo−Mo bond length similar to those of $[Mo(\eta^5\text{-}C_5H_5)(CO)_3]_2$ (3.235(1) Å) and $[Mo(\eta^5\text{-}C_5Me_5)(CO)_3]_2$ (3.278(14) and 3.281(1) Å, $P2_1/c$ and $P2_1/n$ polymorphs),[3p,r] while $[\mathbf{3_2}][B(C_6F_5)_4]_2$ has a shorter W−W bond length than does $[W(\eta^5\text{-}C_5Me_5)(CO)_3]_2$ (3.288(1) Å).[3s]

The fact that the Cr−Cr bond of $[\mathbf{1_2}][B(C_6F_5)_4]_2$ is longer than that of the sterically very hindered $[Cr(\eta^5\text{-}C_5Me_5)(CO)_3]_2$ may be due in part to electrostatic repulsions generated by bringing two positively charged units together although, of course, the covalent radii of the chromium atoms in the cationic complex would also be smaller. Because of steric crowding arising from the metal−metal bonds, the CO ligands are splayed away from the adjacent metal center; consistent with this hypothesis, the M−C−O bonds are not linear but are bent away from the other monomer unit, and in all three complexes the $PMePh_2$ groups of the cyclopentadienylide ligands are orientated away from each other, thus minimizing steric interactions.

In all three cases the P(1)−C(1)−C_5(centroid) angles are <180° such that the phosphorus atoms of the ligands are bent away from the metal centers. The out-of-plane bending observed for these cationic complexes is not observed for the neutral complexes **1**, **2**, and **3**, in which P(1)−C(1)−C_5(centroid) bond angles are nearly linear,[1] but a similar feature is found in the crystal structure of $[Mo(\eta^5\text{-}C_5H_4PMePh_2)(CO)_3I][I]$, in which the P atom is also bent out of the C_5 ring plane.[1] The P(1)−C(1) bonds, used as an indication of the P−C bond order, are elongated in the oxidized species relative to the neutral tricarbonyl starting materials,[1] and again a similar lengthening of the P(1)−C(1) bond is observed in $[Mo(\eta^5\text{-}C_5H_4PMePh_2)(CO)_3I][I]$.[1] The chromium complex has the longest P(1)−C(1) bond distance of 1.784(2) Å, but in all three complexes this bond length approaches those of the P−Ph single bonds.

The C_5 ring is in all cases bound in an η^5 fashion with small variations in the M−C bond distances; carbons C(1), C(2), and C(5) are slightly closer to the metal than are C(3) and C(4). The M−C_5 bond distances are also shorter on average than those observed in the neutral complexes, consistent with the above suggestion of smaller metal covalent radii in the oxidized complexes. The C_5 ring bond lengths and angles do not differ significantly from those of the neutral precursors, and the structures of the borate anions are consistent with other structures reported for this anion.[25]

Nature of the Complexes in Solution: IR, NMR, and MS Data. Having established dimeric structures for all three oxidized species in the solid state, we carried out a series of spectroscopic studies (IR and NMR spectroscopy and ES-MS on solutions, IR spectroscopy on the crystalline solids) to assess the possibility of dissociation of the cationic dimers to monomeric species in solution. The related compounds $[Cr(\eta^5\text{-}C_5H_5)(CO)_3]_2$ and $[Cr(\eta^5\text{-}C_5Me_5)(CO)_3]_2$ do dissociate significantly, while the analogous molybdenum and tungsten dimers do not dissociate thermally at all.[3]

IR spectra were obtained for all three compounds $[M(\eta^5\text{-}C_5H_4PMePh_2)(CO)_3]_2[B(C_6F_5)_4]_2$ (M = Cr, Mo, W) in THF solutions and in the solid state as Fluorolube mulls; all are soluble and stable in THF at room temperature. Interestingly, dilute THF solutions of $[\mathbf{1_2}][B(C_6F_5)_4]_2$ at room temperature are yellow

(25) For several examples see: (a) Yang, X.; Stern, C. L.; Marks, T. J. *Organometallics* **1991**, *10*, 840. (b) O'Connor, A. R.; Nataro, C.; Golen, J. A.; Rheingold, A. L. *J. Organomet. Chem.* **2004**, *689*, 2411.

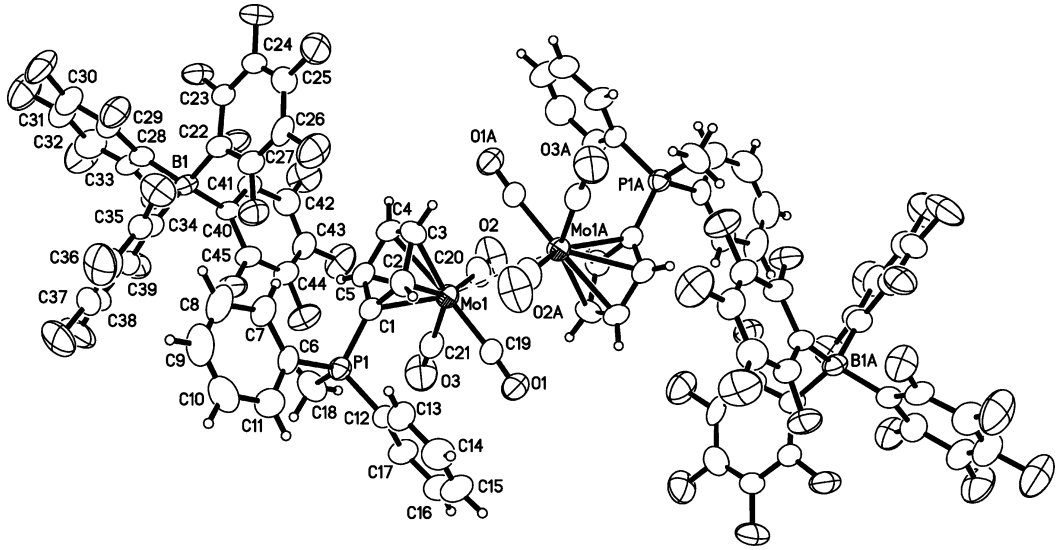

Figure 7. Molecular structure of $[\mathbf{2}_2][B(C_6F_5)_4]_2$.

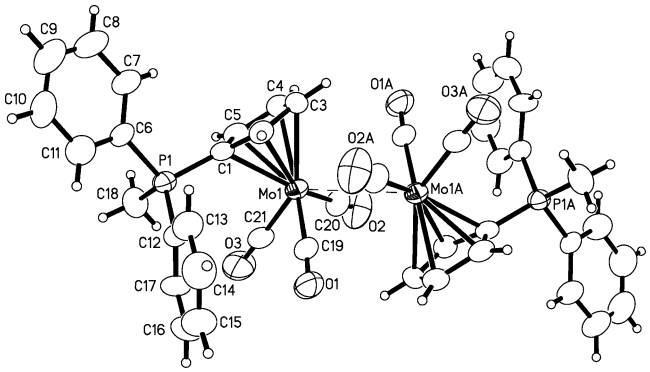

Figure 8. Structure of $[\mathbf{2}_2][B(C_6F_5)_4]_2$ with the anions omitted for clarity.

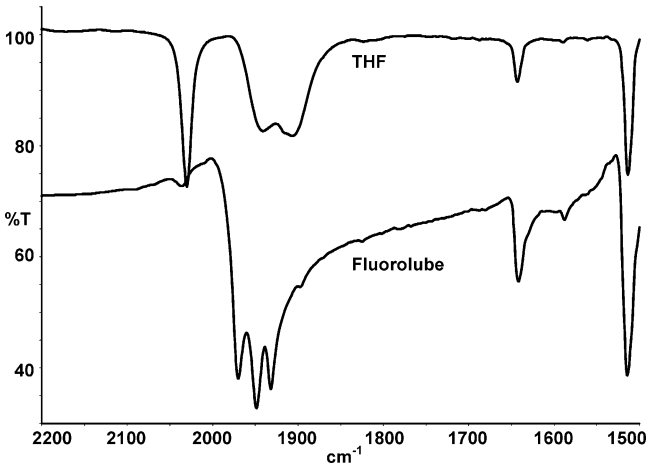

Figure 9. IR spectra of $[\mathbf{1}_2][B(C_6F_5)_4]_2$ in solution and as a mull. The peaks at 1514 and 1643 cm^{-1} are attributed to the $[B(C_6F_5)_4]^-$ anion.

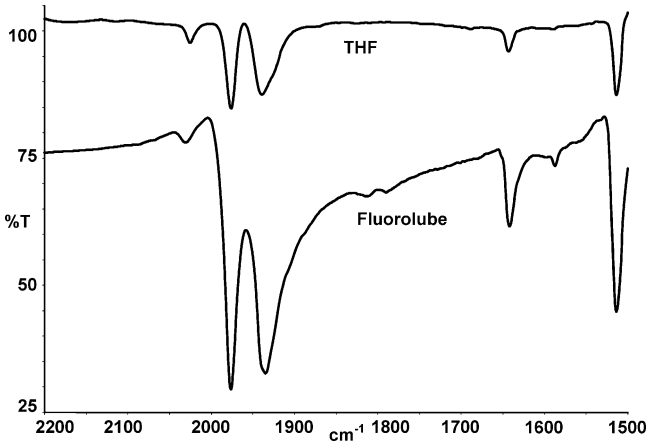

Figure 10. IR spectra of $[\mathbf{2}_2][B(C_6F_5)_4]_2$ in solution and as a mull. The peaks at 1514 and 1643 cm^{-1} are attributed to the $[B(C_6F_5)_4]^-$ anion.

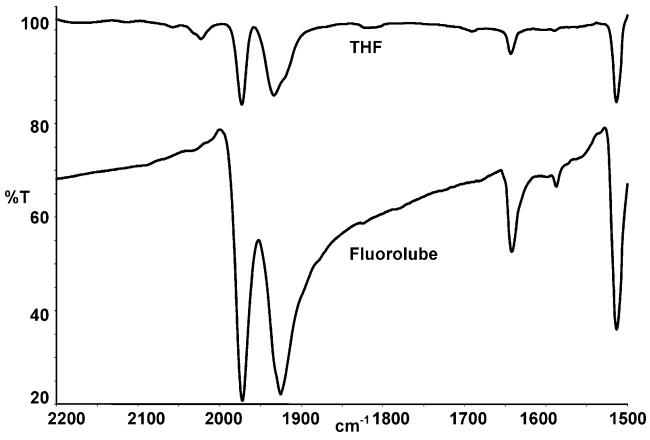

Figure 11. IR spectra of $[\mathbf{3}_2][B(C_6F_5)_4]_2$ in solution and as a mull. The peaks at 1514 and 1643 cm^{-1} are attributed to the $[B(C_6F_5)_4]^-$ anion.

rather than the green of the crystalline dimer, while those of $[\mathbf{2}_2][B(C_6F_5)_4]_2$ and $[\mathbf{3}_2][B(C_6F_5)_4]_2$ are red, the color of the crystalline dimers. Data for the carbonyl stretching modes are listed in Table 4, and the IR spectra are shown in Figures 9−11. As can be seen, while the average frequency of the mull spectrum of the chromium complex is similar to the averages of the solid-state spectra of the molybdenum and tungsten complexes, the peak pattern of the chromium complex differs significantly from those of the other spectra. The difference is probably a result of the chromium complex assuming a different space group (Table 2), since the dimeric dication is the dominant, if not exclusive, form of all three metal complexes in the solid state.

The mull and solution IR spectra of the chromium dimer are markedly different, however, in contrast with the corresponding pairs of solid- and solution-phase spectra of the molybdenum

and tungsten dimers, which are very similar. Indeed, the pattern in the carbonyl stretching region of $[\mathbf{1_2}][B(C_6F_5)_4]_2$ in either THF or CH_2Cl_2 (see below) is very similar to that of the monomeric $Cr(\eta^5\text{-}C_5Me_5)(CO)_3$, for which ν(CO) are observed at 1994 (s) and 1876 (s, br) cm^{-1} in THF and 1994 (s) and 1890 (s, br) in toluene.[3o] Thus the IR data in Table 4 and Figures 2 and 8 are consistent with the presence of the $\mathbf{1}^+$ ion in solution. The carbonyl frequencies are, of course, higher for $\mathbf{1}^+$ than for $Cr(\eta^5\text{-}C_5Me_5)(CO)_3$ as a result of the positive charge in the former. Assuming a double degeneracy of the 1890 cm^{-1} band (ν_{asym}) in $Cr(\eta^5\text{-}C_5Me_5)(CO)_3$, a weighted average shift of +43 cm^{-1} in ν_{CO} is calculated for substitution of the C_5Me_5 ring by $C_5H_4PMePh_2$.

Our observations that the mull IR spectra of $[\mathbf{2_2}][B(C_6F_5)_4]_2$ and $[\mathbf{3_2}][B(C_6F_5)_4]_2$ are nearly identical not only to each other but to the corresponding solution spectra confirm our conclusions based on the electrochemical and spectroelectrochemical evidence that the dimeric ions $\mathbf{2_2}^{2+}$ and $\mathbf{3_2}^{2+}$ are the dominant species in solution as well as in the solid state. Indeed, the IR spectra, which exhibit three strong peaks (one a shoulder) in the region 1900−1980 cm^{-1} in the solution spectra, are very similar in pattern to the spectra of $[Cr(\eta^5\text{-}C_5Me_5)(CO)_3]_2$ in THF (1919, 1902, 1876 cm^{-1}) and toluene (1920, 1900, 1875 cm^{-1}),[3o] although again the frequencies of the cationic complexes are higher. Of particular interest is the rather weak feature at about 2025 cm^{-1} in all the spectra. Being close to the value of the highest energy band of $\mathbf{1}^+$ (2037 cm^{-1}), it must be considered as possibly arising from a small amount of the monomer $\mathbf{2}^+$. We attempted to test this possibility by recording the spectra of $\mathbf{2_2}^{2+}$ at different solution temperatures, but essentially no difference in the relative intensities of the weakest and strongest carbonyl bands was observed between 273 and 310 K in CH_2Cl_2. This result argues for assignment of the 2037 cm^{-1} band to the dimer $\mathbf{2_2}^{2+}$, rather than the monomer $\mathbf{2}^+$, but we cannot rule out the presence, suggested in NMR data (see below), of minor amounts of the monomer radical cation under these conditions.

High-resolution electrospray mass spectra (THF solutions) were also obtained as part of the characterization of the cationic products of the reactions of **1**, **2**, and **3** with $[FeCp_2][B(C_6F_5)_4]$, and for all three systems, the mass spectra exhibited no peaks attributable to dimeric species. The only molecular ions observed were those of the monomeric, 17-electron radicals, $\mathbf{1}^+$, $\mathbf{2}^+$, and $\mathbf{3}^+$, for which the experimental *m*/*z* values differed by only 6.8926, 4.1748, and 3.5448 ppm, respectively, from the calculated *m*/*z* values. Also observed in all cases were excellent isotopic peak distribution matches with the calculated distributions expected for each molecular ion, and an MS−MS experiment of the molecular ion of $\mathbf{1}^+$ revealed a major fragment ion with *m*/*z* of 316, corresponding to the loss of three carbonyls. The conclusions to be drawn from this information in isolation would be that the species in solution are monomeric. However, in view of the overwhelming mass of electrochemical and IR data discussed above, the molybdenum and tungsten dimers must dissociate under the conditions of the mass spectroscopy experiment.

NMR experiments were also carried out to characterize the solution behavior of the oxidized species; these included ^1H, ^{13}C, and ^{31}P NMR experiments and variable-temperature ^1H experiments. A 600 MHz ^1H NMR spectrum of $[\mathbf{1_2}][B(C_6F_5)_4]_2$ in CD_2Cl_2 at 298 K exhibited two very broad C_5H_4 resonances at δ 28.90 ($\Delta\nu_{1/2}$ = 535 Hz) and 13.65 ($\Delta\nu_{1/2}$ = 470 Hz), three somewhat broadened phenyl resonances at δ 7.85, 7.65, and 7.60, and a broad methyl resonance at δ 1.18 ($\Delta\nu_{1/2}$ = 75 Hz); no spin−spin couplings could be observed in any of the resonances. The combination of significant broadening of the ^1H resonances and the very unusual chemical shifts of the C_5H_4 ring hydrogens is consistent with the species in solution being paramagnetic,[26] but an attempt to carry out a variable-temperature experiment failed because of precipitation of $[\mathbf{1_2}][B(C_6F_5)_4]_2$ at lower temperatures.

As shown during our IR studies, however, this complex is very soluble in THF, and ^1H NMR spectra were therefore readily obtained in THF-d_8 over the temperature range 323 to 183 K. No precipitation of either the green dimer or any other solid was noted when the sample was cooled to 183 K, but the solution, which is golden yellow at room temperature, turned green reversibly on cooling. These color changes arise, of course, from reversible interconversion of the green $\mathbf{1_2}^{2+}$ and the yellow $\mathbf{1}^+$.

The ^1H NMR spectrum of $[\mathbf{1_2}][B(C_6F_5)_4]_2$ in THF-d_8 at 298 K was very similar to that observed in CD_2Cl_2, exhibiting two broad C_5H_4 resonances at δ 26.08 ($\Delta\nu_{1/2}$ = 565 Hz) and 13.62 ($\Delta\nu_{1/2}$ = 480 Hz), three broad phenyl resonances in the region δ 8.07−7.66, and a broad P−Me resonance at δ 2.34 ($\Delta\nu_{1/2}$ = 95 Hz). However, lowering the temperature of the sample from 323 to 183 K resulted in major changes, the C_5H_4 resonances broadening somewhat, shifting from δ 23.72 ($\Delta\nu_{1/2}$ = 470 Hz) and 12.85 ($\Delta\nu_{1/2}$ = 385 Hz) at 323 K to δ 28.70 ($\Delta\nu_{1/2}$ = 820 Hz) and 14.10 ($\Delta\nu_{1/2}$ = 795 Hz) at 253 K, and *weakening* relative to the resonance of CH_2Cl_2 added and used as an internal reference. Concomitantly, weak new resonances began to appeared in the "normal" C_5H_4 region, at δ ~5.5−6.2.

By 233 K, the integrated intensities of the two C_5H_4 resonances, now at δ 29.97 and 12.70, had become extremely low and had been replaced by four somewhat broadened resonances of equal intensity, at δ 6.12, 5.96, 5.85, and 5.65. The chemical shifts of the latter four resonances are similar to the C_5H_4 chemical shifts of **1**,[1] **2**,[1] **3**,[1] $\mathbf{2_2}^{2+}$, and $\mathbf{3_2}^{2+}$, supporting the assignments. That there were four separate resonances at this very low temperature rather than the two observed for the other compounds at room temperature probably arises because the cationic dimer is "frozen" in a conformation in which the four H atoms are not equivalent. Indeed, the observed lack of symmetry is consistent with the solid-state structure in which the four ring protons are nonequivalent because of the fixed position of the $PMePh_2$ group; at these low temperatures, slowed rotation of the $PMePh_2$ would be expected and would give rise to magnetic nonequivalence of the C_5H_4 protons.

Simultaneously with the above changes, the P−Me resonance (δ 2.34 at 298 K) decreased in intensity as a new resonance at δ 2.79 appeared and gained in intensity. The original P−Me resonance had disappeared completely at 213 K, leaving only a broadened P−Me resonance at δ 2.89. The latter was not a singlet, but whether the splitting observed was a result of coupling to ^{31}P or of "freezing" of more than one conformation or a combination of both could not be determined. Changes in the closely spaced phenyl resonances as the temperature was lowered were relatively subtle and shed no new light on the situation.

To further investigate the equilibration implied by the ^1H NMR data, the Evans method[27a−c] was used to determine the average magnetic moment of the chromium atoms of $[Cr(\eta^5\text{-}C_5H_4PMePh_2)(CO)_3]_2[B(C_6F_5)_4]_2$ in CD_2Cl_2 at 298 K and in THF over the temperature range 323 to 233 K. The magnetic

(26) Bertini, I.; Luchinat, C.; Parigi, G. *Solution NMR of Paramagnetic Molecules: Applications to Metallobiomolecules and Models*; Elsevier Science B.V.: Amsterdam, 2001.

Table 5. Magnetic Susceptibilities of $[\mathbf{1}_2][B(C_6F_5)_4]_2$ at Different Temperatures

temperature (K)	solvent	μ (μB) ($\pm$0.05)
323	THF-d_8	1.83
308	THF-d_8	1.78
298	THF-d_8	1.80
273	THF-d_8	1.93
253	THF-d_8	1.78
233	THF-d_8	1.46
298	CD_2Cl_2	1.71

susceptibilities were measured using cyclohexane and the residual proton signal of CD_2Cl_2 as references, and diamagnetic corrections and magnetic susceptibilities of solvents were taken from literatures sources.[27] The resulting magnetic moments determined at each temperature are shown in Table 5. As can be seen, the experiments carried out at higher temperatures yielded for both solvents magnetic moments of $\sim$1.8 μ_B, very close to the spin-only value for one unpaired electron.[27] However, the average magnetic moment decreased to 1.46 μ_B on cooling to 233 K, a result consistent with significant dimerization of $\mathbf{1}^+$ to the diamagnetic $\mathbf{1}_2^{2+}$.

These observations extend our conclusions, discussed above and based on visual, electrochemical, and IR spectroscopic evidence, that $\mathbf{1}_2^{2+}$ undergoes reversible dissociation in solution to $\mathbf{1}^+$. However, although our electrochemical investigation of this equilibrium in CH_2Cl_2 at temperatures from ambient to 238 K failed to show any changes that would indicate a degree of dimerization of $\mathbf{1}^+$, the magnetic moment data suggest that significant dimerization occurs in THF at temperatures as high as 233 K. In addition, the low-temperature ^{1}H NMR data suggest that little or no monomer is present at or below 213 K in THF.

Similar observations have been made previously for $[Cr(\eta^5\text{-}C_5H_5)(CO)_3]_2$ and $[Cr(\eta^5\text{-}C_5Me_5)(CO)_3]_2$,[3] of course, but in one sense the $[\mathbf{1}_2][B(C_6F_5)_4]_2$ equilibrium stands in stark contrast to the two neutral monomer−dimer systems. Exchange processes between monomer and dimer for both neutral systems are sufficiently rapid on the NMR time scale that averaged ^{1}H resonances are observed.[3] However, for $[\mathbf{1}_2][B(C_6F_5)_4]_2$, separate C_5H_4 and P−Me resonances are observed over a wide temperature range, and thus monomer−dimer exchange for this system must be slow on the NMR time scale. We are unaware of any other such system where this type of behavior has been observed.

The ^{1}H, ^{31}P, and ^{13}C NMR spectra of $[\mathbf{2}_2][B(C_6F_5)_4]_2$ and $[\mathbf{3}_2][B(C_6F_5)_4]_2$ were obtained in THF-d_8 since these compounds exhibit low solubilities in CD_2Cl_2. For both complexes, the proton and phosphorus resonances were somewhat broadened, possibly evidence for the presence of a small amount of monomeric radicals in the solutions.

Thus the ^{1}H NMR spectrum of $[\mathbf{2}_2][B(C_6F_5)_4]_2$ exhibited a poorly resolved P−Me doublet at δ 2.88, C_5H_4 resonances as broad, featureless bands in the region δ 6.10−6.04 and at δ 5.91, and phenyl resonances in the region δ 7.87−7.72. In no case could ^{1}H−^{1}H coupling be resolved, but variable-temperature experiments conducted in the temperature range 323−213 K showed that the phenyl resonances decoalesced somewhat at 323 K and exhibited three peaks. The C_5H_4 resonances began to overlap as the temperature was lowered. The ^{31}P NMR spectrum exhibited only one resonance, at δ 19.88 and slightly shifted from that of **2** (δ 18.25 in CD_2Cl_2). The ^{13}C NMR spectrum was very similar to that previously reported for $[Mo(\eta^5\text{-}C_5H_4PMePh_2)(CO)_3I][I]$,[1] with nearly identical chemical shifts.

The ^{1}H NMR spectrum of $[\mathbf{3}_2][B(C_6F_5)_4]_2$ at 298 K exhibited two broad phenyl resonances at δ 7.80−7.71, the P−Me resonance as a broad doublet at δ 2.86, and the C_5H_4 resonances as a broad band centered at δ 6.05. Variable-temperature ^{1}H NMR spectra were obtained in the temperature range 198−323 K, and a third phenyl resonance was observed and the C_5H_4 multiplet narrowed above 298 K.

Summary

The group 6 metal complexes $M(\eta^5\text{-}C_5H_4PMePh_2)(CO)_3$ (M = Cr (**1**), Mo (**2**), W (**3**)) are oxidized via one-electron processes, both electrochemically and in bulk by $[FeCp_2][B(C_6F_5)_4]$, to give the corresponding 17-electron, metal-centered radicals $[M(\eta^5\text{-}C_5H_4PMePh_2)(CO)_3]^+$ (M = Cr ($\mathbf{1}^+$), Mo ($\mathbf{2}^+$), and W ($\mathbf{3}^+$)) as the $[B(C_6F_5)_4]^-$ salts. These in turn dimerize to give the metal−metal bonded complexes $[M(\eta^5\text{-}C_5H_4PMePh_2)(CO)_3]_2[B(C_6F_5)_4]_2$ (M = Cr ($\mathbf{1}_2^{2+}$), Mo ($\mathbf{2}_2^{2+}$), and W ($\mathbf{3}_2^{2+}$)), which have been isolated analytically pure and were characterized by IR (solid state and solution) and NMR (^{1}H, ^{13}C, ^{19}F, ^{31}P) spectroscopy, high-resolution mass spectrometry, and crystallographically. The dimers all contain metal−metal bonds that are comparable in length with or longer than the metal−metal bonds in the isoelectronic, neutral η^5-C_5H_5 and η^5-C_5Me_5 compounds, and the metal−metal bond in $\mathbf{1}_2^{2+}$ is the longest nonbridged Cr−Cr bond known. As a result of the apparent weakness of its Cr−Cr bond, $\mathbf{1}_2^{2+}$ dissociates significantly in solution to the paramagnetic, radical cation $\mathbf{1}^+$. The redox behavior of the neutral compounds **1**, **2**, and **3** is qualitatively similar to that of the anionic, isoelectronic analogues $[M(\eta^5\text{-}C_5H_5)(CO)_3]^-$ and $[M(\eta^5\text{-}C_5Me_5)(CO)_3]^-$, with the $[PMePh_2]^+$ substituent exhibiting an electron-withdrawing effect greater than that of the trifluoromethyl group and thus imparting dramatic changes in the redox potentials.

Acknowledgment. We thank the Government of Ontario (Ontario Graduate Scholarship to J.H.B.), Queen's University (Queen's Graduate Award to J.H.B.), the Natural Sciences and Engineering Research Council (Discovery Grant to M.C.B.), and the National Science Foundation (CHE-0411703 to W.E.G.) for funding this research.

Supporting Information Available: One cyclic voltammogram of **1** showing irreversible second anodic wave. Crystallographic details, including figures of $[\mathbf{1}_2][B(C_6F_5)_4]_2$, $[\mathbf{2}_2][B(C_6F_5)_4]_2$, and $[\mathbf{3}_2][B(C_6F_5)_4]_2$, showing complete numbering schemes and thermal ellipsoid figures, and tables of positional and thermal parameters and bond lengths and angles. This material is available free of charge via the Internet at http://pubs.acs.org.

OM700688P

(27) (a) Evans, D. F. *J. Chem. Soc.* **1959**, 2003. (b) Crawford, T. H.; Swanson, J. *J. Chem. Educ.* **1971**, *48*, 382. (c) Sur, S. K. *J. Magn. Reson.* **1989**, *82*, 169. (d) Earnshaw, A. *Introduction to Magnetochemistry*; Academic Press: New York, 1968. (e) Abeles, T. P.; Bos, W. G. *J. Chem. Educ.* **1967**, *44*, 438. (f) Weast, R. C., Lide, D. R., Eds. *CRC Handbook of Chemistry and Physics*, 70th ed.; CRC Press: Boca Raton, FL, 1990; pp E-134−139.